



The following Communications have been judged by at least two referees to be “very important papers” and will be published online at www.angewandte.org soon:

C. D. N. Gomes, O. Jacquet, C. Villiers, P. Thuéry, M. Ephritikhine, T. Cantat*

A Diagonal Approach to Chemical Recycling of Carbon Dioxide: New Organocatalytic Transformation for the Reductive Functionalization of CO₂

X. Zhang, T. J. Emge, K. C. Hultzsich*

A Chiral Phenoxyamine Magnesium Catalyst for the Enantioselective Hydroamination/Cyclization of Aminoalkenes and Intermolecular Hydroamination of Vinyl Arenes

M. A. Newton*, M. Di Michiel, A. Kubacka, A. Iglesias-Juez, M. Fernández-García*

Observing Oxygen Storage and Release at Work under Cycling Redox Conditions: Synergies between Noble Metal and Oxide Promoter

T. Mitsudome, Y. Mikami, M. Matoba, T. Mizugaki, K. Jitsukawa, K. Kaneda*

Design of a Ag@CeO₂ Core–Shell Nanocomposite Catalyst for Complete Chemoselective Reductions

A. Hoffmann, M. T. Woodside*

Signal-Pair Correlation Analysis of Single-Molecule Trajectories

A. Schäfer, M. Reißmann, A. Schäfer, W. Saak, D. Haase, T. Müller*

A Novel Synthetic Route to Triarylsilylium Ions and Their Application in Dihydrogen Activation

P. Berrouard, A. Najari, A. Pron, D. Gendron, P.-O. Morin, J.-R. Pouliot, J. Veilleux, M. Leclerc*

Synthesis of 5-Alkyl[3,4-c]thienopyrrole-4,6-dione-Based Polymers through Direct Heteroarylation

M. Mahut, E. Haller, P. Ghazidezfuli, M. Leitner, A. Ebner, P. Hinterdorfer, W. Lindner, M. Lämmerhofer*

Plasmid DNA Manufacturing: Topology-Selective Chromatography Reveals Plasmid Supercoiling Shifts During Fermentation and Allows Rapid and Efficient Preparation of Topoisomers



“The biggest problem that scientists face is the pursuit of fame and fortune.

If I won the lottery, I would stop applying for grants and concentrate on oxidative coupling research just for fun! ...”

This and more about Aiwen Lei can be found on page 12136.

Author Profile

Aiwen Lei ————— 12136



D. Chen



D. Spiegel



F. Schüth



H. Schwarz

News

Novartis Early Career Award:

D. Y.-K. Chen and D. A. Spiegel — 12137

And also in the News ...

F. Schüth and H. Schwarz — 12137

Books

Statistical Mechanics: Theory and Molecular Simulation

Mark E. Tuckerman

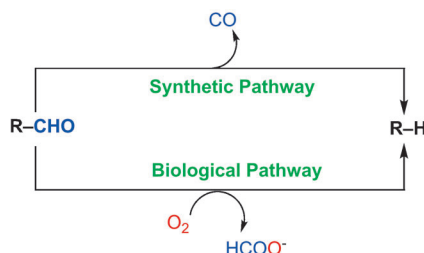
reviewed by S. Alavi — 12138

Highlights

Reaction Mechanisms

T. Patra, S. Manna,
D. Maiti* — 12140–12142

Metal-Mediated Deformylation Reactions:
Synthetic and Biological Avenues

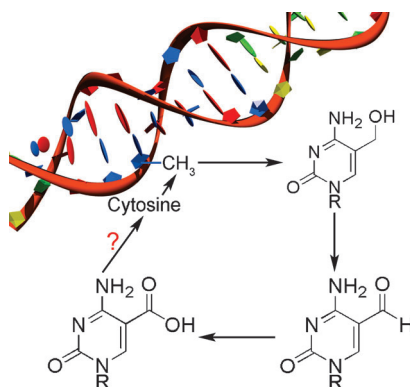


No two ways about it: The title reaction is immensely important in synthesis and biology. Whereas biological systems oxygenate aldehydes to generate formate and alkanes or alkenes, synthetic deformylation reactions primarily rely on rapid oxidative addition into the C(O)–H bond and subsequent rate-determining extrusion of CO.

DNA Demethylation

K. I. Ladwein, M. Jung* — 12143–12145

Oxidized Cytosine Metabolites Offer a
Fresh Perspective for Active DNA
Demethylation

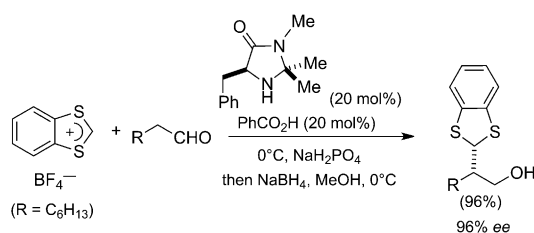


DNA methyltransferases catalyze the transfer of methyl groups to cytosines within DNA. Afterwards, 5-methylcytosine is oxidized to 5-hydroxymethylcytosine. Two further cytosine derivatives, 5-formylcytosine and 5-carboxycytosine, have been discovered recently. The existence of the seventh and eighth nucleobase provides new hints for deciphering the process of active DNA demethylation (see scheme).

Organocatalysis

L. Tak-Tak, H. Dhimane,
P. I. Dalko* — 12146–12147

Asymmetric α Alkylation of Aldehydes:
Efficiency with Elegance



Simple and practical: Direct intermolecular α alkylation reactions by S_N1-type transformations have been developed and

offer flexible and robust routes to major compound classes, for which the direct preparations were unavailable before.

For the USA and Canada:
ANGEWANDTE CHEMIE International
Edition (ISSN 1433-7851) is published weekly
by Wiley-VCH, PO Box 191161, 69451 Wein-
heim, Germany. Air freight and mailing in the
USA by Publications Expediting Inc., 200
Meacham Ave., Elmont, NY 11003. Periodicals

postage paid at Jamaica, NY 11431. US POST-
MASTER: send address changes to *Angewandte
Chemie*, Journal Customer Services, John
Wiley & Sons Inc., 350 Main St., Malden,
MA 02148-5020. Annual subscription price for
institutions: US\$ 11,738/10,206 (valid for print
and electronic / print or electronic delivery); for

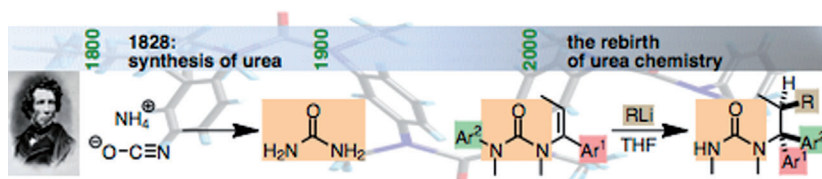
individuals who are personal members of a
national chemical society prices are available
on request. Postage and handling charges
included. All prices are subject to local VAT/
sales tax.

Minireviews

Synthetic Methods

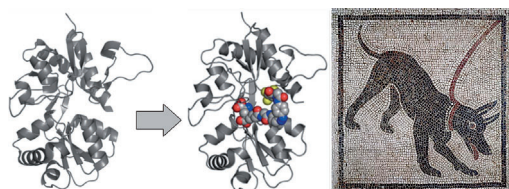
N. Volz, J. Clayden* — 12148–12155

The Urea Renaissance



It's back: This Minireview summarizes the development of urea chemistry during the last few years by taking examples to illustrate each of the themes associated with this renaissance—ureas as lithiation directors, the design of urea-based cata-

lysts and supramolecular structures, the increased reactivity that is characteristic of more hindered ureas, and the electrophilicity disguised within electron-rich aromatic ureas (see picture).



Light of my life: The merger of natural transmembrane proteins with synthetic photoswitches creates hybrid receptors that can be integrated into complex systems and regulated with the precision

that only light provides. This strategy allows for the optical control of single cells, neural systems, and can even be used to control animal behavior.

Reviews

Chemical Genetics

T. Fehrentz, M. Schönberger,
D. Trauner* — 12156–12182

Optochemical Genetics

Communications

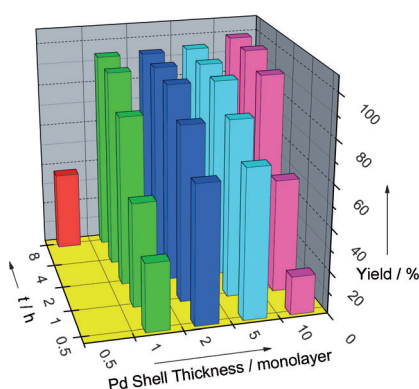
Nanoparticle Catalysis

P. P. Fang, A. Jutand,* Z. Q. Tian,*
C. Amatore* — 12184–12188

Au–Pd Core–Shell Nanoparticles Catalyze Suzuki–Miyaura Reactions in Water through Pd Leaching

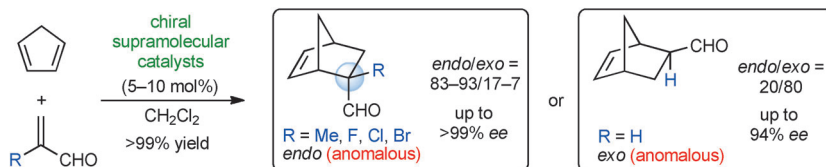


Away from the surface: Novel nanoparticles (NPs) consisting of 16 nm Au cores surrounded by Pd shells of various thicknesses catalyze Suzuki–Miyaura cross-coupling reactions in water at room temperature. NPs having shells of two to five Pd monolayers thick exhibit the highest catalytic activity. Catalysis was attributed to the leaching of Pd species from the NPs through the synergistic action of the carbonate base and the arylboronic acid.



Asymmetric Catalysis

M. Hatano, T. Mizuno, A. Izumiseki,
R. Usami, T. Asai, M. Akakura,
K. Ishihara* 12189–12192



Enantioselective Diels–Alder Reactions with Anomalous *endo/exo* Selectivities Using Conformationally Flexible Chiral Supramolecular Catalysts

Swapped selectivities: The use of tailor-made catalysts results in anomalous *endo/exo* selectivities and high enantioselectivities in the Diels–Alder reactions of cyclopentadiene with different acroleins (see scheme). These supramolecular cat-

alysts are prepared in situ from chiral diols, arylboronic acid, and tris-(pentafluorophenyl)borane, and can discriminate the *re/si* face of the dienophile as well as the *endo/exo* approach of the diene.

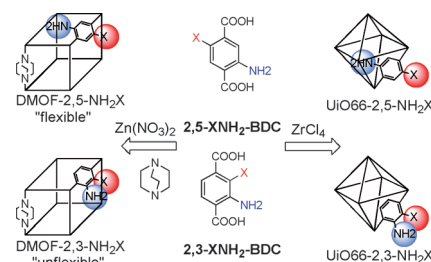
Functional MOFs

M. Kim, J. A. Boissonnault, P. V. Dau,
S. M. Cohen* 12193–12196



Metal–Organic Framework Regioisomers Based on Bifunctional Ligands

Regioisomeric MOFs: A series of bifunctional metal–organic framework (MOF) regioisomers has been produced from amino-halo benzene dicarboxylate ($\text{NH}_2\text{X-BDC}$) ligands. Zr^{IV} - and Zn^{II} -based MOFs were synthesized and for the flexible Zn^{II} -based MOFs, gas sorption properties were dependent on the ligand substitution pattern.



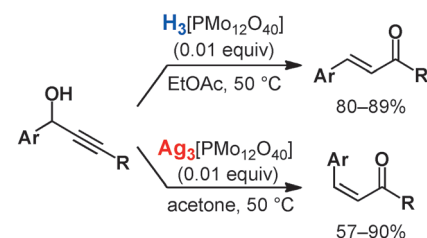
Synthetic Methods

M. Egi, M. Umemura, T. Kawai,
S. Akai* 12197–12200



Heteropoly Compound Catalyzed Synthesis of Both *Z*- and *E*- α,β -Unsaturated Carbonyl Compounds

An *EZ* switch: The cationic species of the heteropoly compounds has a critical impact on the *Z/E* selectivity of the Meyer–Schuster rearrangement of propargyl alcohols (see scheme). The isolation of the thermodynamically unfavorable *Z*- α,β -unsaturated carbonyl compounds is notable. The high *Z* selectivities were obtained at a reaction temperature as high as 50 °C.



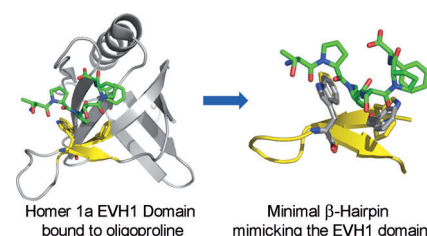
Protein Mimetics

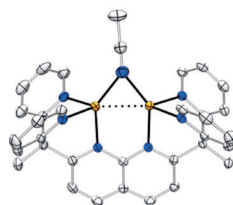
D. J. Wilger, J. H. Park, R. M. Hughes,
M. E. Cuellar,
M. L. Waters* 12201–12204



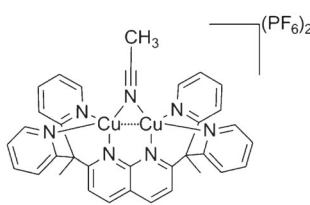
Induced-Fit Binding of a Polypyrrolone Helix by a β -Hairpin Peptide

Form-fitting: The study of a minimal mimic of a protein domain that binds to type II polypyrrolone helices through an aromatic cleft is reported. This binding motif mimics that of protein domains, including those important in disease states such as HIV infection and cancer. This study provides insight into the structure–function relationship in binding as well as quantitative data on the magnitude of π - π interactions relevant to inhibitor design.





Unusual bonding: A ligand system that promotes formation of a rare $\mu\text{-}\eta^1\text{:}\eta^1$ acetonitrile-bridged dicopper(I) complex (see picture) has been developed. The acetonitrile ligand is involved in a three-

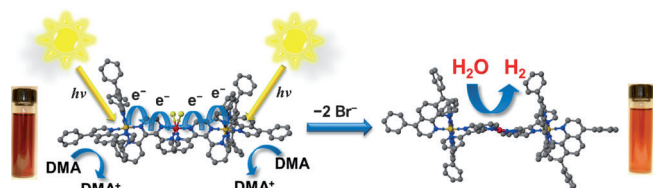


center two-electron bond supported by a cuprophilic interaction. The labile acetonitrile ligand can be substituted with xylol isocyanide or CO.

Electron-Deficient Bonding

T. C. Davenport,
 T. D. Tilley* 12205 – 12208

Dinucleating Naphthyridine-Based Ligand for Assembly of Bridged Dicopper(I) Centers: Three-Center Two-Electron Bonding Involving an Acetonitrile Donor



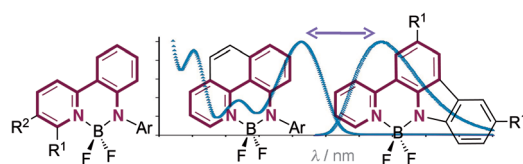
Small changes go a long way: Modification of the terminal ligand to incorporate 4,7-diphenyl-1,10-phenanthroline has generated superior Ru,Rh,Ru photocatalysts (see scheme; ochre Ru, red Rh, blue N, yellow Cl or Br) displaying significantly

enhanced photocatalytic H_2 production from H_2O with long-term functioning: H_2O is reduced to H_2 with over 1300 turnovers per Rh site and a maximum efficiency of 7.3 %.

Photocatalysis

T. A. White, S. L. H. Higgins,
 S. M. Arachchige,
 K. J. Brewer* 12209 – 12213

Efficient Photocatalytic Hydrogen Production in a Single-Component System Using Ru,Rh,Ru Supramolecules Containing 4,7-Diphenyl-1,10-Phenanthroline



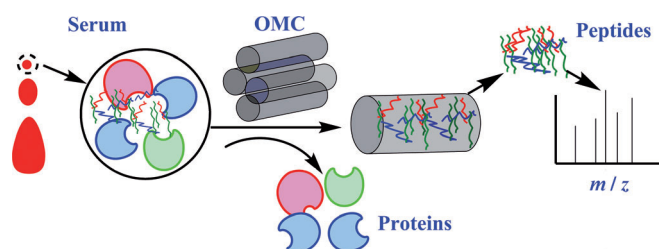
To dye for: Three related families of fluorescent dyes, rigidified by boron difluoride and based on bidentate anilido-pyridyl donor ligands, are reported (see picture). The dyes show quantum yields

up to 0.75 and improved Stokes shifts of > 100 nm relative to the widely employed BODIPY family of dyes. Furthermore, the new dyes are exceptionally photostable and membrane-specific.

Fluorescence

J. F. Araneda, W. E. Piers,* B. Heyne,*
 M. Parvez, R. McDonald - 12214 – 12217

High Stokes Shift Anilido-Pyridine Boron Difluoride Dyes



Size matters: A highly ordered mesoporous carbon material (OMC) was synthesized by a soft-template method, and was applied as an adsorbent for the highly efficient extraction of endogenous pep-

tides from human serum (see scheme). A total of 3402 different peptides were identified from only 20 μL of human serum.

Mesoporous Materials

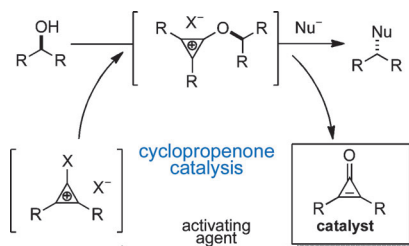
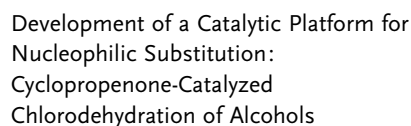
H. Qin, P. Gao, F. Wang, L. Zhao, J. Zhu,
 A. Wang, T. Zhang, R. Wu,*
 H. Zou* 12218 – 12221

Highly Efficient Extraction of Serum Peptides by Ordered Mesoporous Carbon



Synthetic Methods

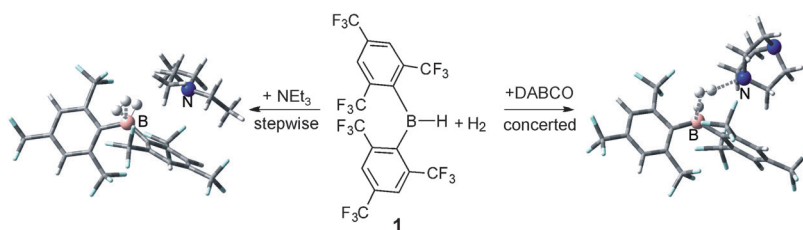
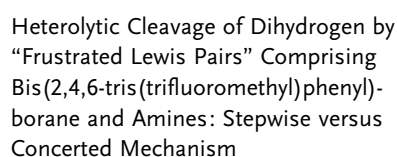
C. M. Vanos,
T. H. Lambert* _____ 12222–12226



Cyclopropenone makes the switch: 2,3-Bis-(*p*-methoxyphenyl)cyclopropenone is a highly efficient catalyst for the chlorodehydration of 20 diverse alcohol substrates (see scheme; X = Cl). With oxalyl chloride as catalytic activator, this nucleophilic substitution proceeded through cyclopropenium-activated intermediates and resulted in complete stereochemical inversion in substrates with chiral centers.

Hydrogen Activation

Z. Lu, Z. Cheng, Z. Chen, L. Weng,
Z. H. Li,* H. Wang* _____ **12227–12231**

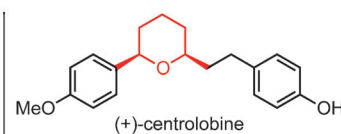
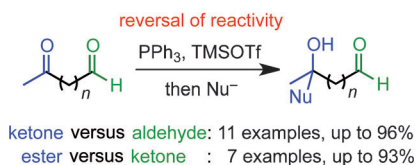
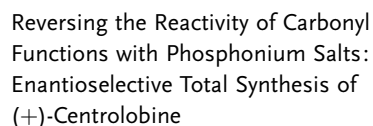


Channeling the frustration: Frustrated Lewis pairs (FLPs) consisting of $\text{Ar}^{\text{F}}\text{BH}$ 1 with NEt_3 or DABCO can activate H_2 under mild conditions. Theoretical calculations suggest two distinct reaction pathways for these two FLPs. For the

“more frustrated” $\text{Ar}^{\text{F}}_2\text{BH}/\text{NEt}_3$, H_2 is activated in a stepwise manner; for the “less frustrated” $\text{Ar}^{\text{F}}_2\text{BH}/\text{DABCO}$, H_2 is activated in a concerted fashion (see scheme).

Carbonyl Reactivity

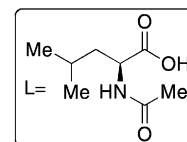
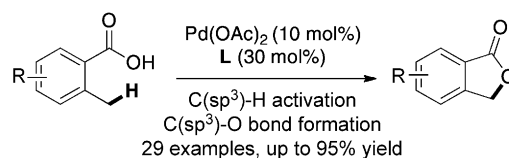
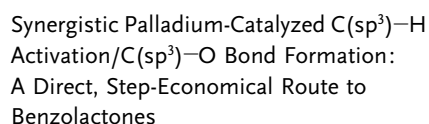
H. Fujioka,* K. Yahata, O. Kubo,
Y. Sawama, T. Hamada,
T. Maegawa _____ **12232–12235**



Step saver: Carbonyl groups with lower reactivities can be transformed in the presence of more reactive ones by treatment with PPh_3 (or PET_3) and TMSOTf prior to the reaction (see scheme; TMS = trimethylsilyl, Tf = trifluoromethanesul-)

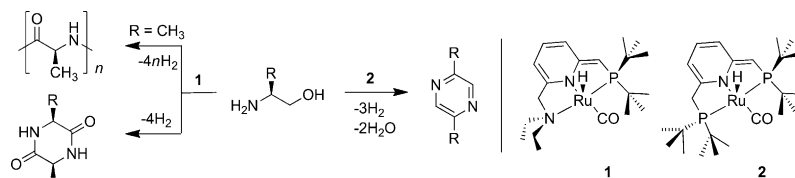
fonyl). This methodology can be applied to reduction and alkylation reactions, and enabled the short asymmetric total synthesis of (+)-centrolobine with the highest overall yield reported to date.

C-H Activation

P. Novák, A. Correa, J. Gallardo-Donaire,
R. Martin* _____ **12236–12239**

Simplified access: Substituted benzolactones can be obtained in one step by a Pd-catalyzed ligand-accelerated C(sp³)-H bond-activation/C(sp³)-O bond-formation protocol. This step-economical approach enables the preparation of ben-

zolidones with a wide variety of functional groups and different substitution patterns. The method is characterized by its simplicity and the avoidance of protecting groups.



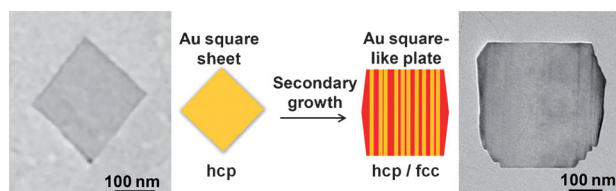
Your choice: The choice of the Ru-pincer-complex catalyst determines if peptides or pyrazines are formed from β -amino alcohols. Use of PNN complex **1** leads to linear poly(alanine) or to cyclic dipeptides,

depending on the R group (see scheme). With the PNP complex **2**, pyrazines are formed. These reactions are homogeneously catalyzed under neutral conditions and are environmentally benign.

Homogeneous Catalysis

B. Gnanaprakasam, E. Balaraman,
Y. Ben-David,
D. Milstein* 12240–12244

Synthesis of Peptides and Pyrazines from β -Amino Alcohols through Extrusion of H_2 Catalyzed by Ruthenium Pincer Complexes: Ligand-Controlled Selectivity



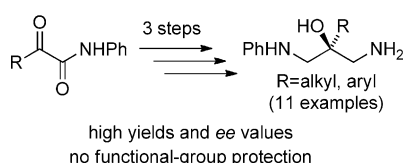
It's hip to be square: Gold square-like plates exhibit alternating hexagonal close-packed (hcp, see picture, yellow) and face-centered cubic (fcc, red) structures in the center and defect-free fcc structures at one pair of the opposite thick edges. They

can be synthesized from Au square sheets in a secondary growth process. For the first time, the hcp-to-fcc phase transformation associated with shape variation in Au nanostructures is demonstrated.

Gold Nanoplates

X. Huang, H. Li, S. Li, S. Wu, F. Boey,
J. Ma, H. Zhang* 12245–12248

Synthesis of Gold Square-like Plates from Ultrathin Gold Square Sheets: The Evolution of Structure Phase and Shape



Three high-yielding steps lead to the formation of chiral 1,3-diaminopropanols from aliphatic and aromatic α -keto amides. In this approach, a nitroaldol reaction, which is catalyzed by Cu-

$(SO_2CF_3)_2$ and the bisoxazolidine ligand **L1**, is followed by two mild reduction reactions (see scheme). Laborious protection and deprotection steps can be avoided by using this method.

Asymmetric Catalysis

H. Xu, C. Wolf* 12249–12252

Asymmetric Synthesis of Chiral 1,3-Diaminopropanols: Bisoxazolidine-Catalyzed C–C Bond Formation with α -Keto Amides



Out of the norm: The first deviation from the *ortho* effect in palladium/norbornene catalysis, as evidenced by the resulting products, is reported (see scheme). DFT calculations indicate that this deviation is likely to originate from a distortion,

caused by specific chelation, in the reductive-elimination pathway from the Pd^{IV} intermediate initially formed. Addition of water restores the normal selectivity, but also it leads to dearomatization.

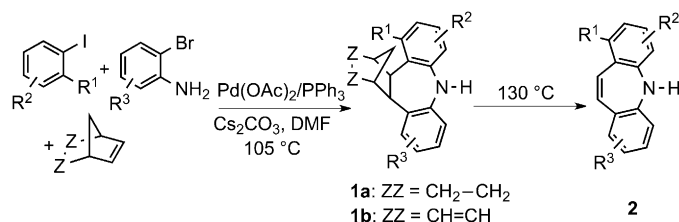
C–C coupling

M.-H. Larraufie, G. Maestri, A. Beaume,
É. Derat, C. Ollivier, L. Fensterbank,
C. Courillon, E. Lacôte,* M. Catellani,
M. Malacria* 12253–12256

Exception to the *ortho* Effect in Palladium/Norbornene Catalysis

Heterocycles

N. Della Ca', G. Maestri, M. Malacria,
E. Derat,* M. Catellani* — 12257–12261



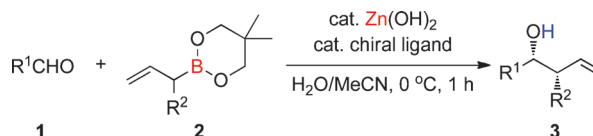
Palladium-Catalyzed Reaction of Aryl Iodides with *ortho*-Bromoanilines and Norbornene/Norbornadiene: Unexpected Formation of Dibenzoazepine Derivatives

Expecting the unexpected: The title reaction leads to satisfactory yields of dihydrodibenzoazepines **1a** from norbornene. The dibenzoazepines **2** can also be accessed from compounds of type **1b** when norbornadiene is used as a reactant.

Theoretical studies show that the reaction represents a chelation-driven deviation from the usual selectivity observed in the presence of *ortho*-substituents on the aryl iodide.

Asymmetric Catalysis

S. Kobayashi,* T. Endo,
M. Ueno — 12262–12265



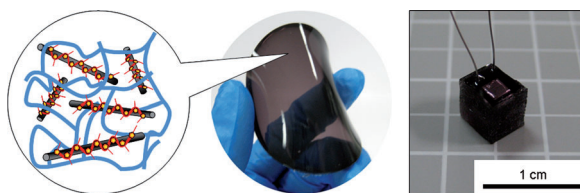
Chiral Zinc-Catalyzed Asymmetric α -Alkylallylation and α -Chloroallylation of Aldehydes

Two birds with one stone: In the presence of Zn(OH)₂ and a chiral bipyridine ligand, racemic α -substituted allylboronates **2** reacted with aldehydes **1** (see scheme) exclusively in an α -addition fashion to

afford various homoallylic alcohols **3** bearing two neighboring stereogenic centers in high yields with high diastereo- and enantioselectivities.

Bioelectronics

E. Miyako,* C. Hosokawa, M. Kojima,
M. Yudasaka, R. Funahashi, I. Oishi,
Y. Hagihara, M. Shichiri, M. Takashima,
K. Nishio, Y. Yoshida — 12266–12270



A Photo-Thermal-Electrical Converter Based On Carbon Nanotubes for Bioelectronic Applications

Electrifying! A device based on carbon nanotubes wrapped with poly(3-hexylthiophene) (and dispersed in poly(dimethylsiloxane)) sheets can effectively convert laser light into thermal energy and subsequently to electricity. The converter

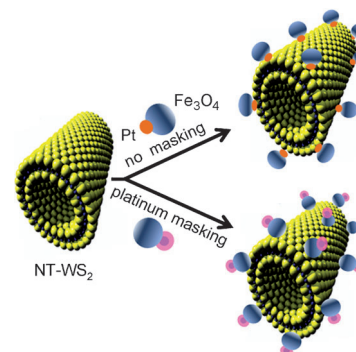
is flexible and extremely compact (see picture), and can be manipulated by using a laser that functions in the wavelength range that can be transmitted through living tissue.

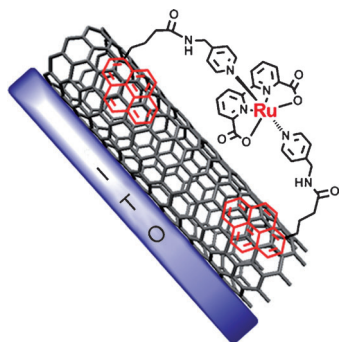
Surface Functionalization

J. K. Sahoo, M. N. Tahir, F. Hoshyargar,
B. Nakhjavan, R. Branscheid, U. Kolb,
W. Tremel* — 12271–12275

Molecular Camouflage: Making Use of Protecting Groups To Control the Self-Assembly of Inorganic Janus Particles onto Metal–Chalcogenide Nanotubes by Pearson Hardness

Hard and soft: Binding of inorganic Pt@Fe₃O₄ Janus particles to WS₂ nanotubes through their Pt or Fe₃O₄ domains is governed by the difference in Pearson hardness: the soft Pt block has a higher sulfur affinity than the harder magnetite face; thus the binding proceeds preferentially through the Pt face. This binding preference can be reversed by masking the Pt face with an organic protecting group.



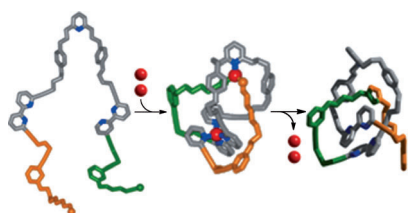


A successful team: A molecular device based on multiwalled carbon nanotubes functionalized by a mononuclear ruthenium catalyst has been shown to split water electrochemically (see picture; ITO = indium tin oxide). The readily prepared electrode showed excellent electrocatalytic activity for the oxidation of water, a high current density, and a low overpotential, and constitutes one step forward in the design of artificial photosynthetic systems.

Water Splitting

F. Li,* B. Zhang, X. Li, Y. Jiang, L. Chen, Y. Li, L. Sun* **12276–12279**

Highly Efficient Oxidation of Water by a Molecular Catalyst Immobilized on Carbon Nanotubes

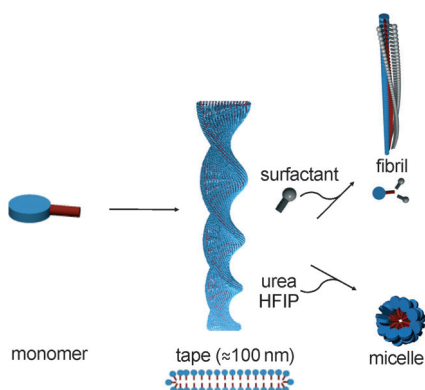


Tying the knot: The marriage of catalysis and coordination chemistry enables two Cu^I ions (red; see picture) to work in partnership for the synthesis of a molecular trefoil knot. One ion entangles an acyclic building block to create a loop in the ligand, and the other gathers the ligand's reactive end-groups, threads the loop, and catalyzes the covalent capture of the knotted architecture by an alkyne-azide "click" reaction.

Chemical Topology

P. E. Barran, H. L. Cole, S. M. Goldup, D. A. Leigh,* P. R. McGonigal, M. D. Symes, J. Wu, M. Zengerle **12280–12284**

Active-Metal Template Synthesis of a Molecular Trefoil Knot



A multisegment amphiphile, made of a gelator and a surfactant, self-assembles into architectures with properties inherited from both segments. By addition of a surfactant, the surfactant segment of the amphiphile is selectively switched off, leading to the formation of fibrils. The addition of urea or hexafluoroisopropyl alcohol (HFIP) switches off the gelator segment, giving micelles.

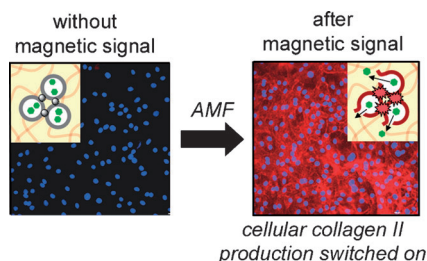
Morphological Transitions

J. Boekhoven, A. M. Brizard, P. van Rijn, M. C. A. Stuart, R. Eelkema, J. H. van Esch* **12285–12289**

Programmed Morphological Transitions of Multisegment Assemblies by Molecular Chaperone Analogues



Crosslinking vesicles with magnetic nanoparticles produced MNPVs, self-assembled "nanopills" that can be "unlocked" by an alternating magnetic field (AMF), releasing chemical messengers stored within the vesicles. When MNPVs are co-immobilized with cells in a hydrogel matrix, exposure to an AMF magnetic signal releases the chemical messengers, which then induce a cellular response.



Magneto-responsive Biomaterials

F. de Cogan, A. Booth, J. E. Gough,* S. J. Webb* **12290–12293**

Conversion of Magnetic Impulses into Cellular Responses by Self-Assembled Nanoparticle-Vesicle Hydrogels

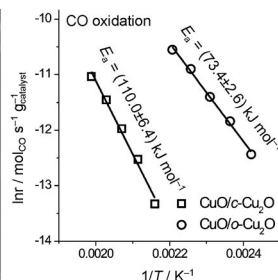
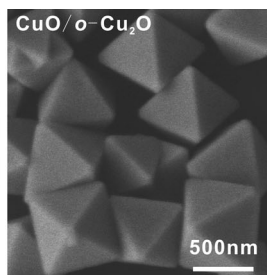
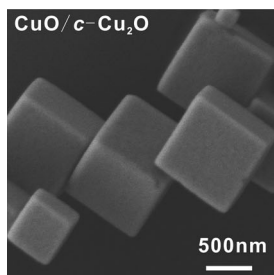


Nanocatalysis

H. Bao, W. Zhang, Q. Hua, Z. Jiang,
J. Yang,* W. Huang* — 12294–12298



Crystal-Plane-Controlled Surface
Restructuring and Catalytic Performance
of Oxide Nanocrystals



Crystal clear: Uniform Cu₂O nanooctahedra (o-Cu₂O) and nanocubes (c-Cu₂O) undergo surface restructuring during CO oxidation for the in-situ formation of catalytically active CuO thin films to give

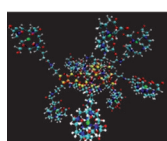
CuO/o-Cu₂O and CuO/c-Cu₂O, respectively (see picture). The structure and catalytic performance of CuO thin films are controlled by the crystal plane exposed on the underlying Cu₂O nanocrystals.

Imaging Agents

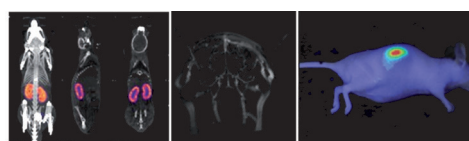
F. Lux, A. Mignot, P. Mowat, C. Louis,
S. Dufort, C. Bernhard, F. Denat,
F. Boschetti, C. Brunet, R. Antoine,
P. Dugourd, S. Laurent, L. V. Elst,
R. Muller, L. Sancey, V. Josserand,
J.-L. Coll, V. Stupar, E. Barbier, C. Rémy,
A. Broisat, C. Ghezzi, G. Le Duc, S. Roux,
P. Perriat,* O. Tillement — 12299–12303



Ultrasmall Rigid Particles as Multimodal
Probes for Medical Applications



Multimodal
imaging
Renal
excretion



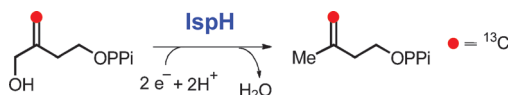
Ultrasmall but multifunctional: Rigid imaging particles that are smaller than 5 nm in size can be obtained in a top-down process starting from a core-shell structure (core = gadolinium oxide;

shell = polysiloxane). They represent the first multifunctional silica-based particles that are sufficiently small to escape hepatic clearance and enable animal imaging by four complementary techniques.

Enzyme Mechanisms

W.-c. Chang, Y. Xiao, H.-w. Liu,*
P. Liu* — 12304–12307

Mechanistic Studies of an IspH-Catalyzed
Reaction: Implications for Substrate
Binding and Protonation in the
Biosynthesis of Isoprenoids



Chosen handle: Mechanistic studies of the IspH-catalyzed reductive dehydroxylation of 4-hydroxy-3-methyl-2-(E)-1-diphosphate (HMBPP) to isopentenyl diphosphate and dimethylallyl diphosphate suggest that both the 4-OH group and the

double bond of HMBPP may contribute to the formation of substrate-IspH complex. Labeling studies now show that the 4-hydroxy group of the substrate plays the dominant role in positioning the substrate in the enzyme active site.

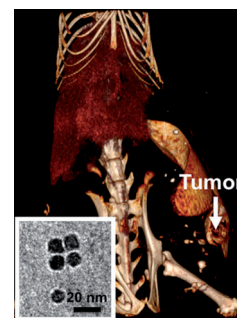
Cancer Imaging

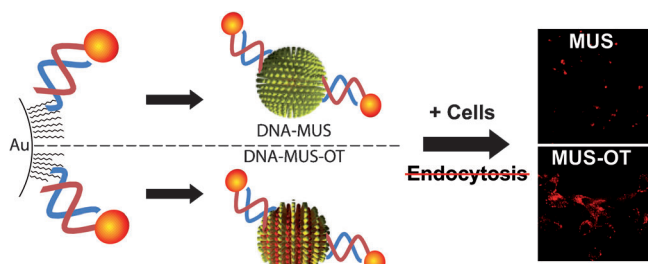
J. M. Kinsella, R. E. Jimenez, P. P. Karmali,
A. M. Rush, V. R. Kotamraju,
N. C. Gianneschi, E. Ruoslahti,
D. Stupack, M. J. Sailor* — 12308–12311



X-Ray Computed Tomography Imaging of
Breast Cancer by using Targeted Peptide-
Labeled Bismuth Sulfide Nanoparticles

Enhanced visualization of breast cancer in X-ray computed tomography was achieved by using Bi₂S₃ nanoparticles of 10 nm diameter modified to display a tumor targeting peptide (LyP-1, CGNKRTRGC). Accumulation within the tumor was increased by 260% over non-labeled nanoparticles.





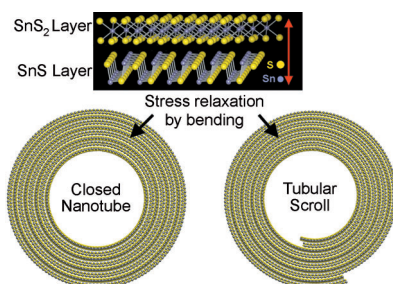
Gold nanoparticles coated with homogeneous (MUS) or “striped” (MUS-OT) ligand shells can be conjugated with double or single stranded DNA, and particles with either ligand configuration

effectively carry DNA into melanoma tumor cells. When endocytosis is inhibited, however, MUS-OT particles continue to mediate DNA delivery, while the delivery ability of MUS particles is abolished.

Delivery Platforms

C. M. Jewell, J.-M. Jung, P. U. Atukorale, R. P. Carney, F. Stellacci,*
D. J. Irvine* — 12312 – 12315

Oligonucleotide Delivery by Cell-Penetrating “Striped” Nanoparticles



Roll ‘em up, move ‘em out: The growth of SnS_2 and SnS_2/SnS nanotubes and nanoscrolls with ordered superstructures is promoted by the relaxation of stress between adjacent SnS_2 and SnS layers. Partial decomposition of the SnS_2 precursor to more sulfur-deficient SnS was manifested in the exfoliation of layers and scrolling. The presence of the two main structures (see picture) was confirmed by HRTEM and Raman spectroscopy.

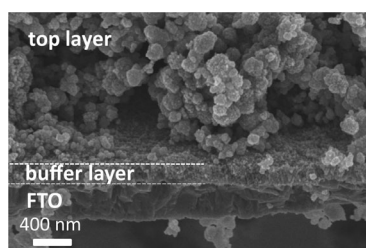
Nanotube Structures

G. Radovsky, R. Popovitz-Biro, M. Staiger, K. Gartsman, C. Thomsen, T. Lorenz, G. Seifert, R. Tenne* — 12316 – 12320

Synthesis of Copious Amounts of SnS_2 and SnS_2/SnS Nanotubes with Ordered Superstructures



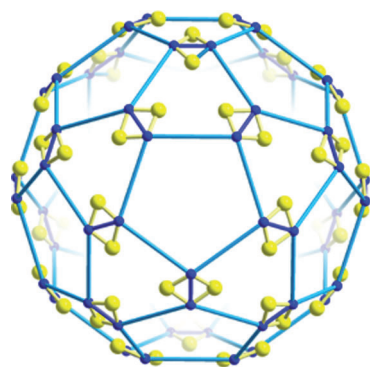
Spray pyrolysis is effective in the formation of a nanoengineered photoanode. An unprecedented photoconversion efficiency of 7.5 % for ZnO -based dye-sensitized cells was achieved on a photoelectrode consisting of polydispersed ZnO aggregates of nanocrystallites over a compact ZnO buffer layer at a firing temperature of 450°C . FTO = fluorine-doped tin oxide.



Dye-Sensitized Solar Cells

N. Memarian, I. Concina, A. Braga, S. M. Rozati, A. Vomiero,*
G. Sberveglieri — 12321 – 12325

Hierarchically Assembled ZnO Nanocrystallites for High-Efficiency Dye-Sensitized Solar Cells



A hard capsule gets soft: The exchange of 60 oxide by 60 sulfide ligands (see picture) in a well-known porous metal-oxide capsule skeleton containing 132 metal atoms changes the interior properties as well as pore sizes, reactivities, flexibilities and affinities to guest molecules.

Porous Capsules

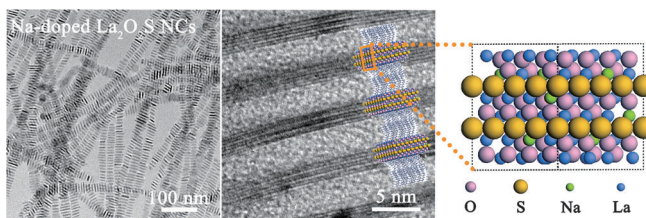
C. Schäffer, A. M. Todea, H. Bögge, E. Cadot, P. Gouzerh, S. Kopilevich, I. A. Weinstock,
A. Müller* — 12326 – 12329

Softening of Pore and Interior Properties of a Metal-Oxide-Based Capsule: Substituting 60 Oxide by 60 Sulfide Ligands



Doped Nanocrystals

Y. Ding, J. Gu, J. Ke, Y.-W. Zhang,*
C.-H. Yan* 12330–12334



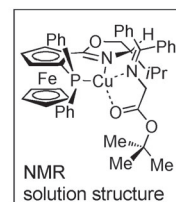
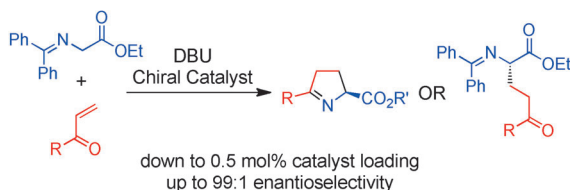
Sodium Doping Controlled Synthesis of Monodisperse Lanthanide Oxysulfide Ultrathin Nanoplates Guided by Density Functional Calculations

Dopant-induced phenomena: Doping with sodium ions can stimulate the formation of monodisperse ultrathin $\text{La}_2\text{O}_2\text{S}$ nanoplates with tunable self-assembled

superstructures (see picture) and robust fluorescence in surfactant solutions by creating oxygen vacancies in the host lattice during sulfurization reactions.

Asymmetric Catalysis

M. Strohmeier, K. Leach,
M. A. Zajac* 12335–12338



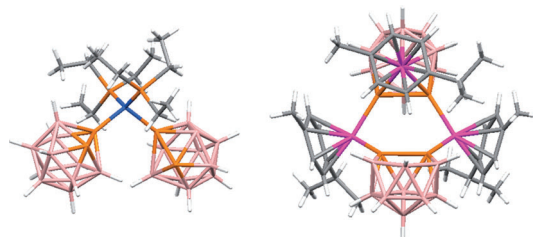
Asymmetric Conjugate Addition of Glycine Derivatives under Copper Catalysis

Coppertunity knocks: An inexpensive, practical, and environmentally benign procedure for the enantioselective addition of glycine derivatives to α,β -unsaturated ketones has been developed (see scheme). By modifying the workup, the

conjugate addition product or a cyclic imine can be accessed. The solution structure of the catalyst–substrate complex is shown to be key to the overall reaction selectivity.

Heteroborane Ligands

R. McLellan, D. Ellis, G. M. Rosair,
A. J. Welch* 12339–12341



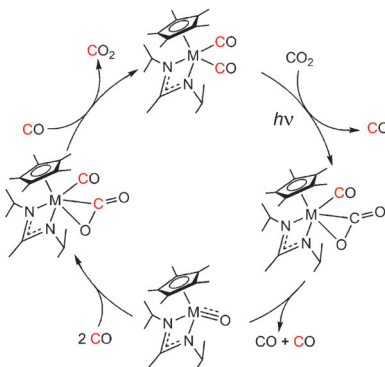
Diphosphaborane and Metalladiphosphaborane: Ligands for Transition-Metal Chemistry

New ligands: The first examples of a neutral heteroborane and a neutral metallaheteroborane acting as simple σ -bound ligands to transition metals are described. In $[\text{HCo}(\text{1,2-closo-P}_2\text{B}_{10}\text{H}_{10})_2]^- (\text{PEt}_3)_2$ (see structure, left) the $\text{P}_2\text{B}_{10}\text{H}_{10}$

ligand coordinates to Co through one P atom, and in $\mu\text{-}[1,2\text{-}\{\text{HRu}(p\text{-cymene})\}_2\text{-7',8'-nido-P}_2\text{B}_9\text{H}_9\text{-3-(}p\text{-cymene)-3,1,2-closo-RuP}_2\text{B}_9\text{H}_9$ (right) both $\text{closo-RuP}_2\text{B}_9$ and $\text{nido-P}_2\text{B}_9$ cages act as bridging $\kappa\text{P}:\kappa\text{P}'$ ligands.

Catalytic Oxidation

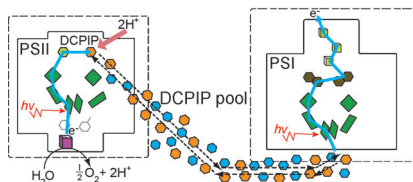
B. L. Yonke, J. P. Reeds, P. Y. Zavalij,
L. R. Sita* 12342–12346



Catalytic Degenerate and Nondegenerate Oxygen Atom Transfers Employing N_2O and CO_2 and a $\text{M}^{\text{II}}/\text{M}^{\text{IV}}$ Cycle Mediated by Group 6 M^{IV} Terminal Oxo Complexes

Green oxidation: A new class of Group 6 metal complexes catalyzes the direct oxidation of isocyanides through non-degenerate oxygen atom transfer (OAT) utilizing N_2O as a chemical oxidant. In addition they serve as photocatalysts for the reversible degenerate OAT between CO and CO_2 (see scheme).

Happily coupled: Photosystem II and photosystem I can be coupled in a sol-gel system so that electron flow can be directly mediated from photooxidized water at the donor side of photosystem II to the highly reducing acceptor side of photosystem I. The electron transfer pathway is set up by addition of the amphipathic quinone analogue 2,6-dichlorophenolindophenol (DCPIP) to the sol-gel mixture to provide a pool of redox carriers (see picture).



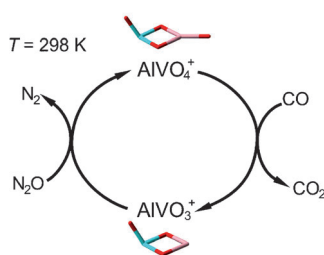
Photosynthesis

F. Kopnov, I. Cohen-Ofri,
 D. Noy* 12347 – 12350

Electron Transport between
 Photosystem II and Photosystem I
 Encapsulated in Sol-Gel Glasses



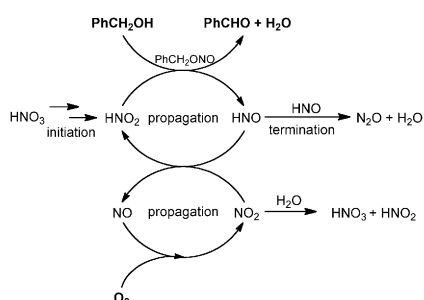
Exhaustive studies: The exact reaction pathway of catalytic conversion of automobile exhaust gases, such as N_2O and CO , into N_2 and CO_2 is still not completely understood. Studying this reaction at room temperature using the bimetallic oxide cluster couple $AlVO_3^+/AlVO_4^+$ in the gas phase shows that the active $M-O^*$ site is located at the Al-bound and not the V-bound oxygen atom (see scheme, Al pink).



Gas-Phase Reactions

Z.-C. Wang, N. Dietl, R. Kretschmer,
 T. Weiske, M. Schlangen,*
 H. Schwarz* 12351 – 12354

Catalytic Redox Reactions in the CO/N_2O
 System Mediated by the Bimetallic Oxide-
 Cluster Couple $AlVO_3^+/AlVO_4^+$



A touch of acid: Catalytic amounts of HNO_3 can trigger the aerobic oxidation of alcohols in the presence of the solid acid amberlyst-15. The desired oxidation cycle, mediated by $(H)NO_x$ species, is in kinetic competition with the detrimental formation of N_2O by HNO dimerization (see scheme). In situ water removal in a gas recirculation reactor increases the reaction rate and the end-conversion by minimizing N_2O formation and increasing the $(H)NO_x$ turnover.

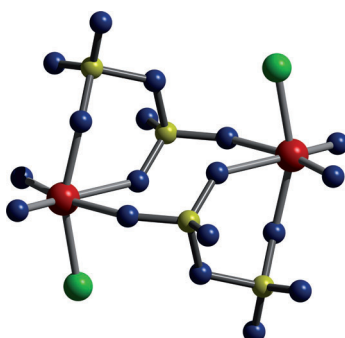
Shuttling Oxygen

C. Aellig, C. Girard,
 I. Hermans* 12355 – 12360

Aerobic Alcohol Oxidations Mediated by
 Nitric Acid



A molecular metal disulfate, $Re_2O_4Cl_2 \cdot (S_2O_7)_2$ forms in the reaction of $ReCl_5$ and oleum (65% SO_3) under harsh conditions. The first of its kind, this unique Re^{VII} compound contains two ReO_2Cl fragments linked by two disulfate groups, leading to C_2 -symmetric molecules (see picture; Re red, O blue, S yellow, Cl green).



Molecular Disulfate

U. Betke, W. Dononelli, T. Klüner,
 M. S. Wickleder* 12361 – 12363

$ReO_2Cl(S_2O_7)_2$, a Molecular Disulfate



Supporting information is available
 on www.angewandte.org
 (see article for access details).



A video clip is available as Supporting
 Information on www.angewandte.org
 (see article for access details).



This article is available
 online free of charge
 (Open Access)

Sources

Product and Company Directory

You can start the entry for your company in "Sources" in any issue of *Angewandte Chemie*.

If you would like more information, please do not hesitate to contact us.

Wiley-VCH Verlag – Advertising Department

Tel.: 0 62 01 - 60 65 65

Fax: 0 62 01 - 60 65 50

E-Mail: MSchulz@wiley-vch.de

Service

Spotlight on Angewandte's

Sister Journals _____ 12 132 – 12 134

Vacancies _____ 12 129

Preview _____ 12 365

Corrigendum

Hydrogen-Independent Reductive Transformation of Carbohydrate Biomass into γ -Valerolactone and Pyrrolidone Derivatives with Supported Gold Catalysts

X. L. Du, L. He, S. Zhao, Y. M. Liu,
Y. Cao,* H. Y. He, K. N. Fan **7815–7819**

Angew. Chem. Int. Ed. **2011**, 50

DOI: 10.1002/anie.201100102

The authors of this Communication have noticed an error in the Supporting Information. In Figure S1 e, the same TEM image was inadvertently used as in Figure S1 a. The correct Figure S1 e is shown below. This error does not affect the interpretation of results in the Communication. The authors sincerely apologize for this oversight and any inconvenience it may have caused.

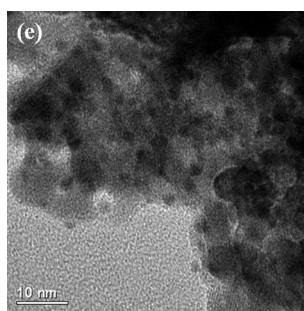
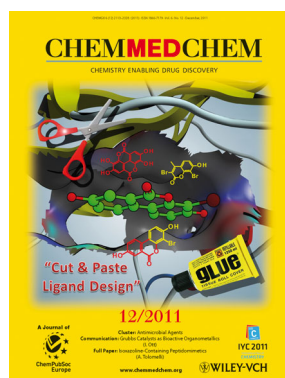


Figure S1. TEM image of e) Au/ZrO₂-VS (after five runs).

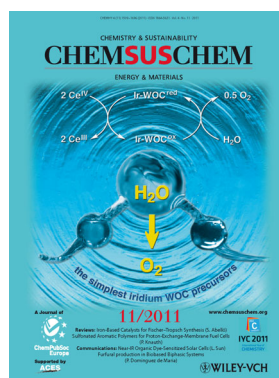
Check out these journals:



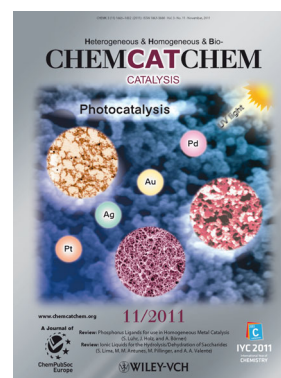
www.chemasianj.org



www.chemmedchem.org



www.chemsuschem.org



www.chemcatchem.org